Stat3 promotes directional cell migration by regulating Rac1 activity via its activator βPIX

Terk Shin Teng[1,*], Baohong Lin[1,‡], Ed Manser[1], Dominic Chi Hiung Ng[1,§] and Xinmin Cao[1,2,¶]

[1]Institute of Molecular and Cell Biology, A*STAR (Agency for Science, Technology and Research), Singapore 138673
[2]Department of Biochemistry, National University of Singapore, Singapore 117597

*Present address: Singapore Immunology Network, A*STAR, Singapore 138648
‡Present address: Department of Haematology, National University Hospital, Singapore 119074
§Present address: Department of Biochemistry and Molecular Biology, Molecular Science and Biotechnology Institute, University of Melbourne, Melbourne, Victoria, Australia 3010
¶Author for correspondence (mcbcaoxm@imcb.a-star.edu.sg)

Accepted 8 September 2009
Journal of Cell Science 122, 4150-4159 Published by The Company of Biologists 2009
doi:10.1242/jcs.057109

Summary

Stat3 is a member of the signal transducer and activator of transcription family, which is important for cytokine signaling as well as for a number of cellular processes including cell proliferation, anti-apoptosis and immune responses. In recent years, evidence has emerged suggesting that Stat3 also participates in cell invasion and motility. However, how Stat3 regulates these processes remains poorly understood. Here, we find that loss of Stat3 expression in mouse embryonic fibroblasts leads to an elevation of Rac1 activity, which promotes a random mode of migration by reducing directional persistence and formation of actin stress fibers. Through rescue experiments, we demonstrate that Stat3 can regulate the activation of Rac1 to mediate persistent directional migration and that this function is not dependent on Stat3 transcriptional activity. We find that Stat3 binds to βPIX, a Rac1 activator, and that this interaction could represent a mechanism by which cytoplasmic Stat3 regulates Rac1 activity to modulate the organization of actin cytoskeleton and directional migration.

Supplementary material available online at
http://jcs.biologists.org/cgi/content/full/122/22/4150/DC1

Key words: Actin, βPIX, Cell migration, Rac1, Stat3

Introduction

The signal transducers and activators of transcription (STATs) were identified as latent cytoplasmic transcription factors that are activated by cytokines and growth factors to mediate essential cellular processes such as cell growth, proliferation and immune responses (Darnell et al., 1994). Upon induction, STAT proteins are phosphorylated on a specific tyrosine residue at the C-terminus, which is required for the subsequent dimerization and nuclear translocation, where STATs function as transcription factors to regulate target gene expression (Darnell, 1997). The STAT family consists of seven members in mammals, with Stat3 being most pleiotropic in terms of the biological functions mediated. Notably, Stat3 has also drawn attention because of its capacity to induce cellular transformation and tumorigenesis (Bromberg et al., 1998). Aberrant Stat3 activation has been subsequently reported in a variety of human cancers (Bowman et al., 2000). Initially, it was suggested that Stat3 contributes to progression of cancers by mediating cell proliferation and anti-apoptosis (Levy and Lee, 2002; Calo et al., 2003). Recently, there is emerging evidence on the importance of Stat3 in regulating cell migration, motility and invasion in both physiological and pathological situations. The first indication came from conditional knockout of Stat3 in the mouse. Deletion of Stat3 in keratinocytes compromised the wound-healing process in skin, and cell migration in cultured cells (Sano et al., 1999). A similar role of Stat3 in regulating cell migration has also been found in mouse embryonic fibroblasts (MEFs) and keloid-derived fibroblasts (Lim et al., 2006; Ng et al., 2006). In *Drosophila*, the JAK-STAT pathway has been shown to activate migratory and invasive behavior of ovarian epithelial cells in ovarian development (Silver et al., 2005). Stat3 has also been found to control cell movement during zebrafish gastrulation (Yamashita et al., 2002). In agreement with this finding, Stat3-knockout mice exhibit embryonic lethality during gastrulation (Takeda et al., 1997). Furthermore, promotion of tumor invasion and metastasis by Stat3 has been widely reported in various cancers, including ovarian carcinoma, melanoma and bladder, pancreatic and prostate cancers (Wei et al., 2003; Silver et al., 2004; Xie et al., 2004; Itoh et al., 2006; Abdulghani et al., 2008). These data suggest that regulation of cell movement could be a fundamental function of Stat3. However, exactly how Stat3 regulates cell migration remains largely unknown.

Cell migration is crucial for many biological processes, including embryonic development, wound healing and immune surveillance, and it also contributes to cell invasion and tumor metastasis (Lauffenburger and Horwitz, 1996; Raftopoulou and Hall, 2004). Directional cell migration is a tightly coordinated process that is initiated by the ability of a cell to adhere, polarize and coordinate its actin cytoskeleton to form membrane protrusion, which extends to form a lamellum at the leading edge to dictate the direction of movement (Ridley et al., 2003). Consequently, localized actin polymerization at the lamellipodium is required for the generation of propulsive force to mediate forward movement (Pollard and Borisy, 2003). As the cell extends its lamellipodium and forms new adhesion contacts, it contracts its cell body to move forward over the new adhesion contacts and detaches itself at the rear.

The Rho family of small GTPases, in particular Cdc42, Rac1 and RhoA, modulates the dynamic of actin and microtubule cytoskeleton to control directional migration (Nobes and Hall, 1995; Raftopoulou and Hall, 2004). The Rho GTPases function as molecular switches by cycling between an inactive, GDP-bound

state and an active GTP-bound state to regulate cytoskeletal reorganization. Rac1 promotes ruffling and protrusions of the membrane to form the lamellipodia as well as focal complex formation (Ridley et al., 1992; Nobes and Hall, 1995). Cdc42 mediates filopodia formation and regulates cell polarity (Kozma et al., 1995; Nobes and Hall, 1995). RhoA regulates stress fiber formation and focal adhesion assembly (Ridley and Hall, 1992). However, the functions of Cdc42, Rac1 and RhoA on cytoskeletal reorganization and cell migration are not mutually exclusive. The interplay and balance of Rho GTPase signaling is crucial for directional migration (Nobes and Hall, 1999; Sander et al., 1999). The activity of these Rho GTPases is regulated by guanine nucleotide exchange factors (GEFs), which promote GDP to GTP exchange (Rossman et al., 2005), and GTPase-activating proteins (GAPs), which promote intrinsic GTP hydrolysis (Bernards, 2003). Given the complexity of Rho GTPase signaling, any perturbation in the regulation of the Rho GTPases would invariably affect cytoskeletal organization and cell migration.

In this study, we address the question of how Stat3 regulates cell migration. We report here that a loss of Stat3 expression results in a random mode of migration and Stat3 is required to maintain directional persistence during migration. We demonstrate that this function of Stat3 is independent of its transcriptional activity and occurs via Stat3 regulation of Rac1 activity. βPIX (PAK-interacting exchange factor or ARHGEF7) was first identified as a PAK1-binding protein (Bagrodia et al., 1998; Manser et al., 1998) and subsequently shown to mediate Rac1 activation (ten Klooster et al., 2006). We show that Stat3 can bind to βPIX via its C-terminus and that this interaction could represent a mechanism, in which Stat3 modulates Rac1 activity to regulate the organization of actin cytoskeleton and directional migration.

Results

Loss of Stat3 expression reduces directional persistence in cell migration

In this study, we used wild type (WT) and Stat3-deficient murine embryonic fibroblasts (ΔSt3 MEFs) (Costa-Pereira et al., 2002), as a model system to investigate the role of Stat3 in regulating cell migration. Previously, we have reported that migrating ΔSt3 MEFs exhibited a reduced rate of wound closure in an in vitro wound-healing assay (Ng et al., 2006). Further characterization revealed that the ΔSt3 MEFs migrated randomly, with some single cells at the wound front moving out of the monolayer during migration, whereas the WT MEFs migrated smoothly as a sheet of cells (Fig. 1A; supplementary material Movies 1 and 2). The F-actin organization of migrating cells at the wound front showed that the broad lamella of WT MEFs was replaced by multiple protrusions in ΔSt3 MEFs (Fig. 1B). These observations suggested that the ΔSt3 MEFs could be compromised in either directional migration or cell-cell adhesion, or both. To investigate this further, we examined the migratory behavior of WT and ΔSt3 MEFs during random migration, which allowed us to characterize the intrinsic ability of individual cell to migrate in the absence of external directional cues and quantify the speed and directionality of migration independent of cell-cell adhesion. Cells were seeded sparsely on fibronectin-coated plates and monitored by time-lapse microscopy. We observed that the WT MEFs displayed a classical polarized phenotype represented by the formation of a dominant lamella at the front and

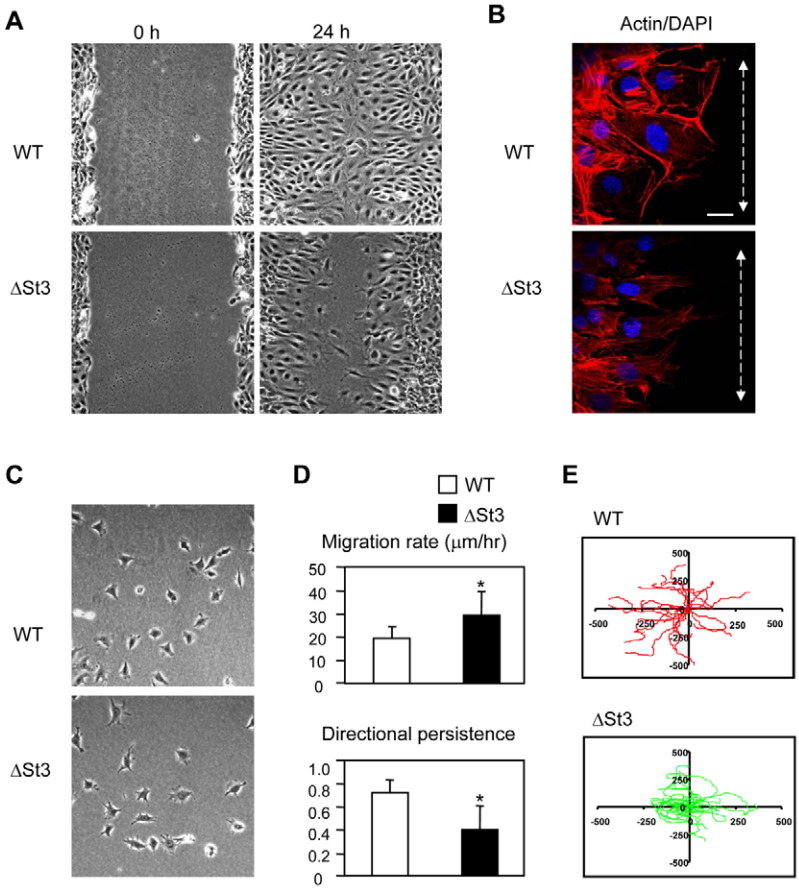

Fig. 1. Loss of Stat3 expression affects directional migration. (A) ΔSt3 MEF exhibits altered morphology during migration. Phase-contrast images of WT and ΔSt3 MEFs at 0 and 24 hours after wounding. (B) Staining of the actin cytoskeleton in migrating cells. Confluent monolayers of WT and ΔSt3 MEFs were wounded and then fixed and stained with DAPI and Alexa Fluor 488-conjugated phalloidin after 5 hours. Dotted line indicates direction of the wound. Scale bar: 20 μm. (C) ΔSt3 MEFs exhibit a non-polarized phenotype during migration. Phase-contrast images of WT and ΔSt3 MEFs collected during random migration. (D) Analysis of migration rate and directional persistence by random migration assay. WT and ΔSt3 cells were plated sparsely and monitored by time-lapse microscopy for 16 hours. Rate and persistence of migration were quantified as described in Materials and Methods. Data represent means ± s.e.m. (error bars) of 30 cells pooled from at least three independent experiments. **P*<0.001. (E) Migration tracks of WT and ΔSt3 MEFs. Tracks from 20 random cells from D were plotted using Excel.

a narrow trailing edge at the rear (Fig. 1C; supplementary material Movie 3). By contrast, ΔSt3 MEFs consistently exhibited a non-polarized phenotype with several membrane protrusions around the cell periphery during migration (Fig. 1C). These membrane protrusions were short lived and retracted frequently (supplementary material Movie 4). We then quantified the rate and persistence of migration for both cell types. In contrast to the observation that ΔSt3 MEFs were slower in wound closure, the ΔSt3 MEFs migrated significantly faster than WT cells (Fig. 1D, top panel, $*P<0.001$). This difference can be explained because ΔSt3 MEFs were compromised with respect to directional persistence of migration (Fig. 1D, bottom panel, $*P<0.001$). Graphical representations of the migratory paths clearly show the random and irregular pattern of ΔSt3 MEFs (Fig. 1E).

Impaired actin networks in ΔSt3 MEFs

Polarized actin polymerization has a key role in the maintenance of directional migration (Cory and Ridley, 2002). Based on our earlier observations that migrating ΔSt3 MEFs have an altered actin cytoskeleton (Fig. 1B), we asked whether abnormal migratory behavior of the ΔSt3 cells parallels the abnormal F-actin organization. The ΔSt3 cells have less actin stress fibers (Fig. 1B, Fig. 2A). To investigate whether the reduction of stress fiber formation in the ΔSt3 MEFs was due to a compromise in actin polymerization, we treated the WT and ΔSt3 MEFs with phorbol 12-myristate 13-acetate (PMA), a potent inducer of actin remodeling, and analyzed their ability to reorganize the actin cytoskeleton. Surprisingly, the ΔSt3 MEFs were capable of undergoing actin polymerization induced by PMA as indicated by the actin staining in the membrane ruffles (Fig. 2B). This indicates that the reduction of stress fiber formation in the ΔSt3 MEFs could be caused by other factors.

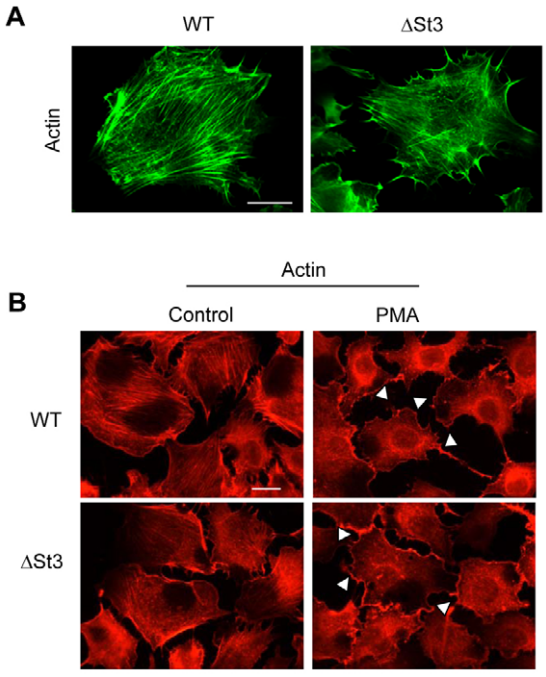

Fig. 2. Effect of Stat3 on actin cytoskeleton. (A) Organization of the actin cytoskeleton in WT and ΔSt3 MEFs. WT and ΔSt3 MEFs were fixed and stained with Texas-Red-conjugated phalloidin. Scale bar: 20 μm. (B) Analysis of PMA-induced reorganization of actin cytoskeleton. WT and ΔSt3 MEFs were plated overnight on fibronectin-coated coverslips before being treated with or without PMA for 1 hour. Cells were then fixed and stained with Texas-Red-conjugated phalloidin. Membrane ruffles are labelled with arrows. Scale bar: 20 μm.

Previously, we have reported that the organization of the microtubule cytoskeleton is disrupted in the ΔSt3 cells (Ng et al., 2006). Therefore, we sought to determine whether there is any connection between the disorganized microtubule network and the reduced content of stress fibers. We observed that in WT MEFs, treatment of either microtubule-destabilizing drug nocodazole or microtubule-stabilizing drug taxol did not affect the formation of stress fibers (supplementary material Fig. S1); similarly, the decreased microtubule stability induced by nocodazole or the increased in microtubule stability induced by taxol in ΔSt3 MEFs, did not significantly alter actin stress fiber levels (supplementary material Fig. S1). We conclude that the defect in the actin cytoskeleton of the ΔSt3 cells is not directly related to the change in organization of microtubules.

ΔSt3 MEFs display elevated Rac1 activity

Rac1 activity is essential for lamella formation to mediate persistent migration (Cory and Ridley, 2002). Based on the phenotype displayed by the ΔSt3 MEFs during migration, Rac1 activity was assayed in the ΔSt3 MEFs. Consistent with the increased migration, steady state levels of GTP-Rac1 were higher in ΔSt3 MEFs than in control cells (Fig. 3A), whereas the levels of GTP-RhoA were similar in both cell lines (Fig. 3B). To confirm the general effect of Stat3 in suppressing GTP-Rac1, we assayed the ΔSt3 MEFs under conditions that promote Rac1 activation. An increase of Rac1 activity was observed throughout the time points measured after monolayer scratching (Fig. 3C), and during cell attachment and spreading (Fig. 3D).

To confirm this correlation between Stat3 expression and the regulation of Rac1 we took a well-studied epithelial line (MCF-7) and knocked down Stat3 expression using siRNA. The stable downregulation of Stat3 expression in these cells again increased the levels of GTP-Rac1 but not GTP-RhoA (Fig. 3E); thus Stat3 serves to regulate the extent of Rac1 activation.

Rac1 activity is the determinant of persistence in directional migration, and affects the actin cytoskeleton

The perturbation of Rac1 by altering the level of Stat3 can be detected by alteration of the total level of GTP-Rac1. Notably, a change in the overall level of GTP-Rac1 has been shown to influence the intrinsic migratory behavior of fibroblasts (Pankov et al., 2005). To investigate the relationship between directional persistence and GTP-Rac1 levels in ΔSt3 MEFs, we asked whether the elevation of GTP-Rac1 could bring about a loss of directionality in cell migration. To examine this, we generated a pool of WT MEFs stably expressing either GFP or GFP-G12V-Rac1 (constitutively active mutant) by retroviral transduction and characterized their migratory behavior using the random migration assay. Time-lapse movies revealed that the control WT MEFs expressing GFP migrated in a polarized and persistent fashion (supplementary material Movie 5). By contrast, the expression of GFP-G12V-Rac1 resulted in behavior whereby these cells formed multiple membrane protrusions and migrated more randomly (supplementary material Movie 6). Analysis indicated that constitutive active Rac1 reduced directional persistence whereas the overall speed of migration increased (Fig. 4A,B; $*P<0.001$). In addition, the expression of GFP-G12V-Rac1 impaired lamellipodia formation. In contrast to control WT MEFs expressing GFP, which tend to form a dominant lamella, the expression of GFP-G12V-Rac1 in WT MEFs resulted in multiple

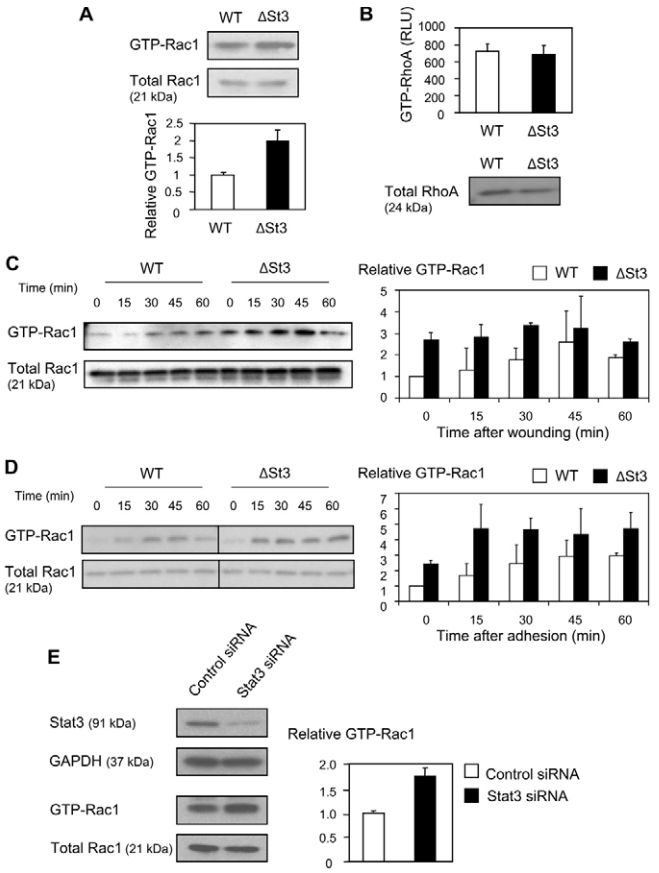

Fig. 3. ΔSt3 MEFs exhibit elevated Rac1 activation during integrin-mediated adhesion and migration. (A) Cells were plated on fibronectin-coated plates overnight before being lyzed, and the amount of GTP-Rac1 was determined by western blotting. Level of GTP-Rac1 was quantified by densitometry, normalized against the total amount of Rac1 present in the cell lysate, and expressed as relative fold GTP-Rac1 compared with WT MEFs. Data represent means ± s.e.m. (error bars), *n*=3. (B) The level of RhoA in WT and ΔSt3 MEFs was determined using the RhoA G-LIZA kit. The level of GTP-RhoA is represented as luminescence units (RLU). Western blotting of the total cell lysate (TCL) with anti-RhoA served as loading control. Data represent means ± s.e.m. (error bars), *n*=3. (C) Analysis of Rac1 activity during wound-induced cell migration. Confluent monolayer of WT and ΔSt3 MEFs were wounded and lyzed at the indicated time points to assay for Rac1 activity. Data represent means ± s.e.m. (error bars), *n*=2. (D) Analysis of Rac1 activity during cell spreading. Cells were assayed for Rac1 activity at the time indicated after replating onto fibronectin. Time 0 refers to cells in suspension. Data represent means ± s.e.m. (error bars), *n*=3. (E) Knockdown of Stat3 expression in MCF-7 cells increases Rac1 activation. The level of Rac1 activity was examined in the MCF-7 cells stably expressing Stat3 siRNA or control siRNA. The level of Stat3 expression was determined by western blot. The membrane was reprobed with anti-GAPDH to serve as loading control. Data represent means ± s.e.m. (error bars), *n*=3. One western blot is shown in panels A-E as a representative result.

membrane protrusions (supplementary material Fig. S2). The similarities in migratory characteristics exhibited by WT MEFs expressing GFP-G12V-Rac1 and ΔSt3 MEFs indicate that inappropriate elevation of Rac1 activity can produce increased lamellipodia number, thereby leading to a loss of directional persistence during migration.

It is well established that RhoA promotes stress fiber formation (Ridley and Hall, 1992), whereas Rac1 tends to decrease stress fiber formation by promoting its disassembly (Albertinazzi et al., 1999). Accordingly, we asked whether the reduction of stress fibers in the ΔSt3 MEFs could be attributed to a defect in RhoA signaling or an elevation of Rac1 activity. Although the stable expression of GFP-G14V RhoA (constitutively active mutant) in WT MEFs increased stress fiber formation compared with control WT MEFs expressing GFP, ΔSt3 MEFs expressing GFP-G14V RhoA still appeared similar to control ΔSt3 MEFs expressing GFP with very little stress fiber formation (Fig. 4C). However, the expression of GFP-T17N Rac1 (dominant-negative mutant) in ΔSt3 MEFs was able to increase stress fiber formation (Fig. 4C).

The role of Rac1 in downregulating stress fiber formation was reported to be dependent on the activation of its effector, PAK (Sanders et al., 1999; Zhao et al., 2000). Upon activation by Rac1, PAK can phosphorylate and inactivate the myosin light chain kinase, thus leading to a decrease in cell contractility as a result of the lack of myosin light chain phosphorylation by myosin light chain kinase (Sanders et al., 1999). This in turn leads to the reduction of stress fiber formation. To demonstrate the cooperation between Rac1 and PAK in downregulating stress fiber formation, we expressed an auto-inhibitory domain (AID) of PAK, which has been shown to inhibit the kinase activity of PAK (Zhao et al., 1998), in ΔSt3 MEFs and analyzed its effect on stress fiber formation. We observed that stress fiber formation was increased in the ΔSt3 MEFs expressing GFP-PAK AID compared with control ΔSt3 cells expressing GFP (Fig. 4D). Collectively, these results indicate that elevation of Rac1 activity in ΔSt3 MEFs is responsible for the loss of stress fiber formation.

Stat3 rescues defective cell migration and abnormal Rac1 activity independently of transcriptional activity

To clarify how Stat3 loss alters cell migration, we examined whether Stat3-dependent transcriptional activity was required to maintain the normal behavior of MEFs in migration assays. We reintroduced either GFP-WT Stat3 or a GFP-Y705F Stat3 into the ΔSt3 line via retrovirus-mediated transduction. The Y705 is essential for Stat3 phosphorylation, dimerization and translocation into the nucleus upon activation (Kaptein et al., 1996). The level of GTP-Rac1 in these rescued cells was similar, with GFP-WT Stat3 or GFP-Y705F Stat3 versus the control ΔSt3 cells expressing GFP (Fig. 5A). Next, we tested whether GFP-Y705F Stat3 could also rescue the migratory defect in ΔSt3 MEFs. As shown in Fig. 5B, the presence of GFP-Y705F Stat3 rescued MEF wound closure and migration to a comparable level as the control WT MEFs expressing GFP. It was noticed in the ΔSt3 MEFs expressing GFP, that although some single cells at the wound front seemed to move out of the monolayer at a fast rate, the majority of the cells still moved more slowly than the WT MEFs expressing GFP and the GFP-Y705F Stat3 rescued cells. In addition, in contrast to the multiple membrane protrusions observed in the GFP-expressing ΔSt3 MEFs, the expression of GFP-Y705F Stat3 in ΔSt3 MEFs was able to restore normal lamella formation (supplementary material Fig. S2). Furthermore, in the random migration assay, expression of GFP-Y705F Stat3 in the ΔSt3 MEFs not only reduced the rate of migration, but also significantly increased the directional persistence (Fig. 5C,D; **P*<0.001). The migratory rescue can be observed clearly in supplementary material Movies 7-9). Together, these data demonstrate a mechanism for regulation of Rac1-mediated processes by Stat3 that is independent of its transcriptional activity.

Stat3 interacts with βPIX, a Rac1/Cdc42 GEF

A question remains as to how Stat3 affects Rac1 activation to regulate cell migration. Rac1 has been reported to interact with Stat3

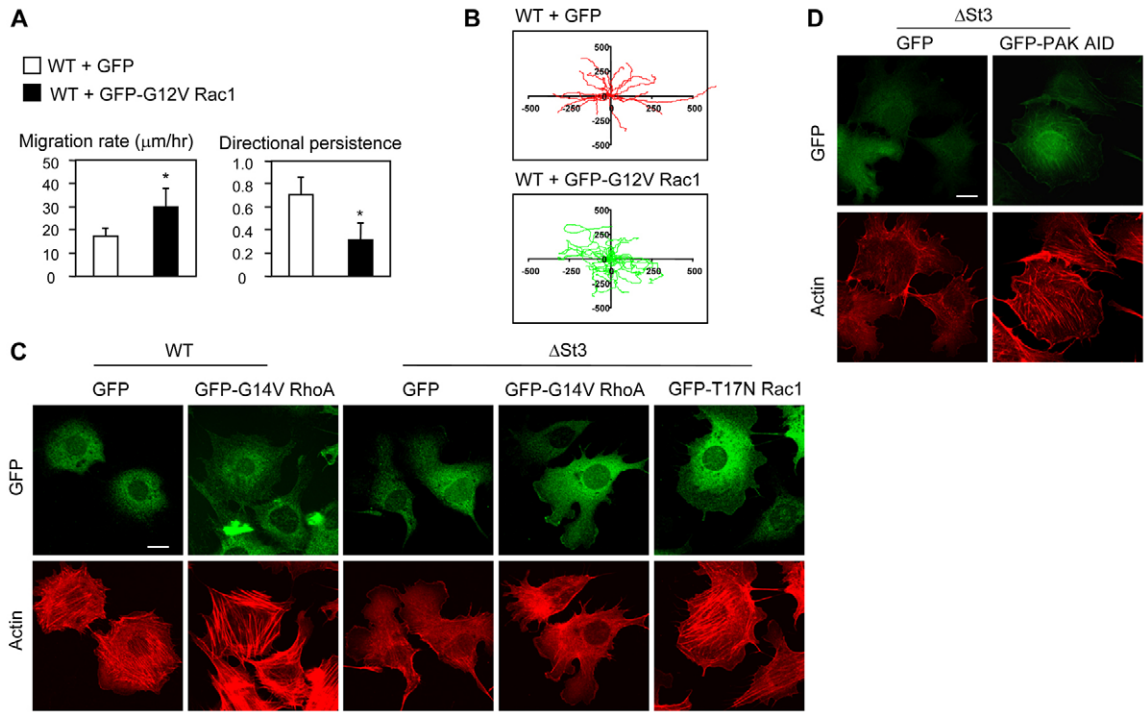

Fig. 4. Increase of Rac1 activity promotes random migration. (A) Stable WT MEFs expressing either GFP or GFP-G12V Rac1 were pooled and analyzed using the random migration assay to determine the rate and persistence of migration. Data represent means ± s.e.m. (error bars) of 30 cells pooled from at least three independent experiments. **P*<0.001. (B) Migration tracks of control WT MEFs expressing GFP and WT MEFs expressing GFP-G12V Rac1. Tracks of 20 random cells from A were plotted using Excel. (C) Expression of GFP-G14V RhoA mutant increases formation of stress fibers in WT MEFs but not ΔSt3 MEFs. WT and ΔSt3 MEFs stably expressing either GFP, GFP-G14V RhoA or GFP-T17N Rac1 were fixed and stained with anti-GFP (green) and Texas-Red-conjugated phalloidin (red). Increase of stress fiber formation in ΔSt3 MEFs was only observed after expression of GFP-T17N Rac1. Scale bar: 20 μm. (D) Inhibition of PAK activity in ΔSt3 MEFs promotes stress fiber formation. ΔSt3 cell stably expressing either GFP or GFP-auto-inhibitory domain (AID) of PAK were fixed and stained with anti-GFP (green) and Texas-Red-conjugated phalloidin (red) to visualize the actin cytoskeleton. Scale bar: 20 μm.

(Simon et al., 2000). Thus, this interaction could represent a possible model to explain Stat3 regulation on Rac1 activity. However, we have not been able to detect any interaction between Stat3 and Rac1 (data not shown), which is similar to other reports (Debidda et al., 2005).

βPIX, which is a ubiquitous Rac1/Cdc42 GEF, can bind and locally activate such GTPases to allow local targeting of Rac1 to focal adhesion and membrane ruffles during cell spreading (Manser et al., 1998). Therefore, we asked whether Stat3 could interact with βPIX to affect the regulation of Rac1. Since βPIX is the exclusive isoform in HeLa cells (Manser et al., 1998), we looked for the presence of Stat3 in immunoprecipitates of βPIX. Indeed, we observed that endogenous Stat3 coimmunoprecipitated with βPIX antibody but not with control rabbit IgG (Fig. 6A). The region of Stat3 that interacts with βPIX encompassed the C-terminal section (residues 600-770), which consists of an SH2 domain as well as the transactivation domain and analysis revealed that the Stat3 SH2 domain alone is sufficient to mediate the interaction with βPIX (Fig. 6B,C). Thus, this seems to suggest that the Stat3 interaction with βPIX could be phosphorylation dependent. Although a recent study has shown that βPIX can undergo tyrosine phosphorylation (Chang et al., 2007), we could not establish any association between βPIX phosphorylation and Stat3 interaction, because we found that the lysis of cells in the presence or absence of sodium orthovanadate, a protein phosphotyrosyl phosphatase inhibitor, did not affect the interaction of Stat3 with βPIX (data not shown). The key function for βPIX is as a scaffold to link the kinase PAK to GIT1, a focal adhesion and centrosomal adaptor protein (Bagrodia et al., 1998; Manser et al., 1998; Zhao et al., 2000). The function of βPIX is dependent on homo-oligomerization, which is probably a trimer (Schlenker and Rittinger, 2009), mediated by the coiled-coil domain (Kim et al., 2001; Koh et al., 2001). To investigate whether Stat3 interaction with βPIX requires other βPIX-interacting proteins, we assayed the ability of both WT and Y705F Stat3 to bind various βPIX mutants (Fig. 6D). Binding of both the WT and Y705F mutant was unaffected by the W43P/W44G βPIX SH3 mutant that does not bind PAK, as well as a mutant (I539P/E540G) that cannot bind GIT1 (Fig. 6E). In addition, both WT and Y705F Stat3 could bind to the truncated βPIX (residues 1-555), which lacks the coiled-coil domain. Together, these results indicate that the βPIX interaction with Stat3 does not require binding to its main partners PAK and GIT1.

Functional analysis of the Stat3-βPIX interaction

To test whether the interaction between Stat3 and βPIX is relevant for their respective functions, we first investigated whether βPIX expression modulates Stat3 signaling. We transfected HEK293T cells with HA-βPIX and analyzed the phosphorylation and transcriptional activity of Stat3 in the transfected cells after stimulation with oncostatin M (OSM). We found that overexpression of βPIX did not significantly affect Stat3 phosphorylation at Y705 or its transcriptional activity (Fig. 7A,B).

We then asked whether the Stat3 interaction with βPIX could represent a mechanism to regulate Rac1 activation. To test this, we

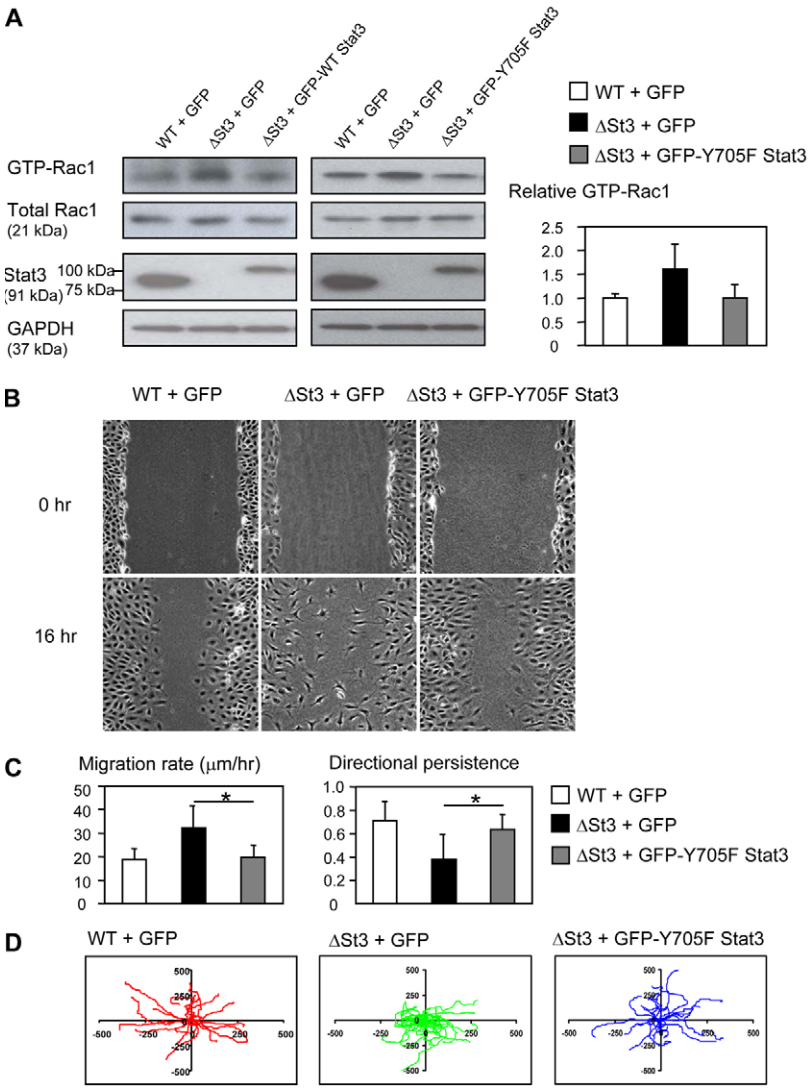

Fig. 5. Expression of GFP-Y705F Stat3 in ΔSt3 MEFs reduces Rac1 activation and rescues migration defects. (A) For rescue experiments, ΔSt3 MEFs were infected with retroviruses expressing either GFP-WT Stat3 or GFP-Y705F Stat3, whereas for control, WT and ΔSt3 MEFs were infected with retroviruses expressing GFP alone. Stable cell lines were established and Rac1 activity was analyzed (left panels) as described in Fig. 3A. Data represent means ± s.e.m. (error bars), n=3 (right panel). The expression levels of GFP-WT Stat3 or GFP-Y705F Stat3 were confirmed with western blot using anti-Stat3 antibody. The membrane was reprobed with anti-GAPDH to serve as loading control. (B) Expression of GFP-Y705F Stat3 in ΔSt3 cells restores migration during wound healing. Phase-contrast images of control WT MEFs, control ΔSt3 MEFs and rescued GFP-Y705F MEFs were taken at 0 and 16 hours after wounding. (C) Expression of GFP-Y705F Stat3 in ΔSt3 cells promotes persistent directional migration. Similarly, the three different populations of MEFs were analyzed by random migration assay as described in Fig. 1D. Data represent means ± s.e.m. (error bars) of 30 cells pooled from at least three independent experiments. *P<0.001. (D) Migration tracks of control WT MEFs, control ΔSt3 MEFs and rescued GFP-Y705F Stat3 MEFs. Tracks of 20 random cells from experiment reported in C were plotted using Excel.

overexpressed HA-βPIX in the presence or absence of either FLAG-WT Stat3 or FLAG-Y705F Stat3 in HEK293T cells, and assayed the effect of Stat3 on βPIX-induced Rac1 activation. Overexpression of βPIX led to an increase in Rac1 activity during cell adhesion on fibronectin (Fig. 7C, lane 2). However, the level of Rac1 activation induced by βPIX was significantly reduced in the presence of either FLAG-WT Stat3 or FLAG-Y705F Stat3 (Fig. 7C, lanes 3 and 4). This indicates that Stat3 can attenuate βPIX-induced activation of Rac1, independently of its transcriptional activity. However, if Stat3 exerts its effect on the Rac1 activation through βPIX, downregulation of βPIX in the ΔSt3 MEFs should reduce the Rac1 activity. We found that the suppression of βPIX by shRNA in ΔSt3 MEFs indeed resulted in a decrease of Rac1 activity during cell spreading (Fig. 7D). Thus, inappropriate Rac1 activation in the ΔStat3 MEFs during cell spreading and migration could involve a failure to properly regulate βPIX.

Discussion

Involvement of Stat3 in the regulation of cell migration in embryonic development and cancer metastasis has been clearly demonstrated, but its effect and mechanism have not been well defined. In the past, the major assay utilized was in vitro wound-healing, and the results were controversial. Although most reports showed that Stat3 deficiency compromised cell migration (Sano et al., 1999; Kira et al., 2002; Ng et al., 2006), opposing results have also been reported (Debidda et al., 2005). The wound-healing assay measures the rate of collective cell movement in which it is difficult to observe the migratory behavior of individual cells. In this study, we carefully characterized the migratory behavior of Stat3-deficient cells in wound healing, as well as in random migration to monitor the individual moving cells. For the first time, we revealed that the major migratory defects of ΔSt3 MEFs are a loss of directional persistence, rather than a decrease of velocity, and a failure in lamella formation (Fig. 1). This finding might explain why the ΔSt3 MEFs exhibit a reduction in the rate of migration during the wound-healing process. Given that Stat3-knockout mice exhibit embryonic lethality during gastrulation (Takeda et al., 1997), where coordinated directional migration is a crucial event, our findings indicate the functional importance of Stat3 in embryonic development by regulating directional cell migration. The phenotypes we observed in Stat3-deficient cells also led us to uncover the possible underlying mechanisms.

The Rho GTPases are central regulators of the actin cytoskeleton dynamics during directional migration (Ridley, 2001; Raftopoulou

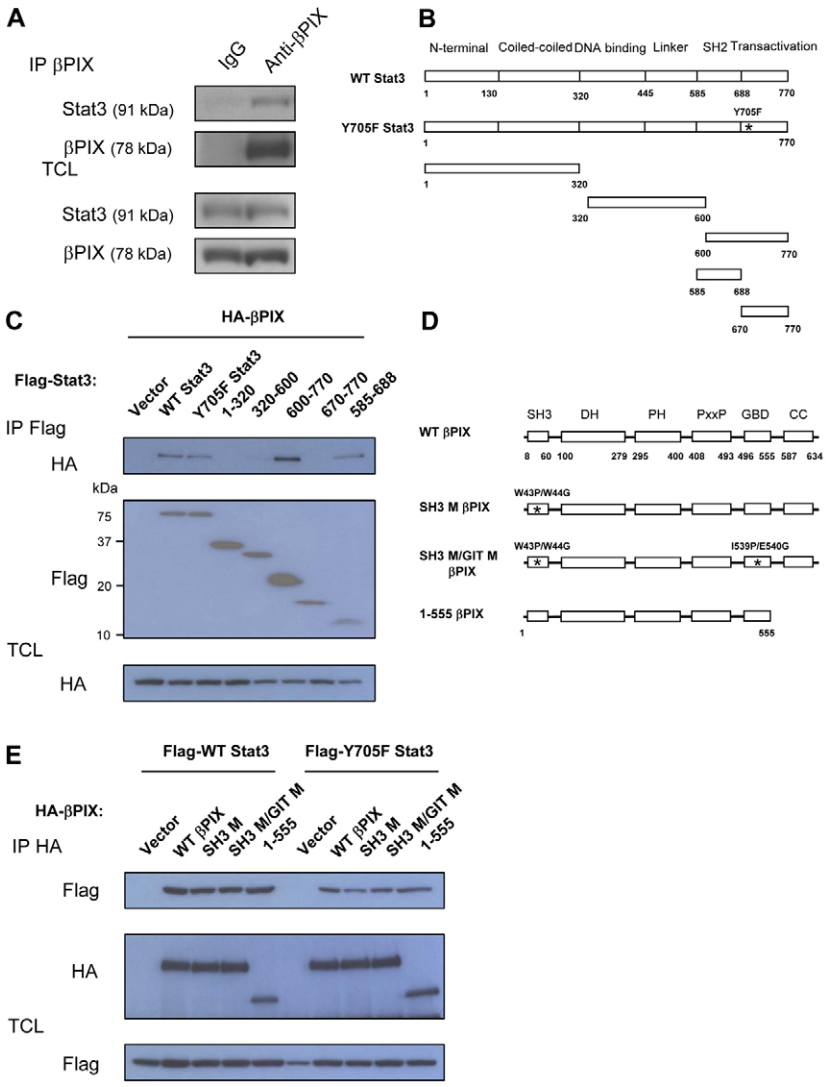

Fig. 6. Stat3 interacts with βPIX. (A) Endogenous interaction of Stat3 with βPIX. Immunoprecipitation (IP) was performed in HeLa cells with βPIX antibody or normal rabbit IgG antibody as a control. The immunoprecipitates were analyzed by western blotting using Stat3 or βPIX antibody (top and second panels). Total cell lysates (TCL) were subjected to western blot analysis using Stat3 or βPIX antibody (third and bottom panels). (B) Schematic representation of the domain organization of Stat3 to illustrate the various truncated form of Stat3 mutants used for mapping studies. (C) Stat3 binds to βPIX via its C-terminal region. HEK 293T cells were cotransfected with HA-βPIX and the various FLAG-Stat3 constructs as indicated. IP was performed using FLAG antibody and the association of HA-βPIX was detected by western blotting using HA antibody (top panel). The precipitated Stat3 was detected using anti-FLAG antibody (middle panel). The expression level of HA-βPIX in TCL was detected with anti-HA antibody (bottom panel). (D) Schematic representation of the domain organization of βPIX and the βPIX mutants used. βPIX contains a SH3 domain, a dbl homology (DH) domain, a Pro-rich region (PxxP), a GIT1-binding domain (GBD) and a coiled-coil domain (CC). SH3 M βPIX, SH3 domain mutant of βPIX (W43P/W44G); SH3 M/GIT M, SH3 domain mutant and GIT1 binding-deficient mutant of βPIX. Asterisk indicates the respective amino acid substitutions. 1-555, βPIX mutant lacking the coiled-coil domain. (E) HEK 293T cells were cotransfected with either FLAG-WT Stat3 or FLAG-Y705F Stat3 with the various HA-βPIX constructs as indicated. Immunoprecipitation was performed using anti-HA antibody and association of the various βPIX constructs was detected by western blotting using anti-FLAG antibody (top panel). The amounts of immunoprecipitated HA-βPIX were detected by anti-HA antibody (middle panel). Expression of FLAG-WT Stat3 and FLAG-Y705F Stat3 in TCL is shown in the bottom panel.

and Hall, 2004). Rac1, specifically, drives actin polymerization to promote lamellipodium formation at the leading edge of migrating cells. Therefore, the precise spatial regulation of Rac1 activity is paramount during cell migration. Indeed, numerous studies have shown that deregulation of Rac1 activity results in impaired cell migration (Pankov et al., 2005; Pratt et al., 2005; Katoh et al., 2006). Interestingly, by using overexpression and siRNA approaches in a variety of cell types, including fibroblasts and epithelial cells, Pankov and co-workers (Pankov et al., 2005) demonstrated that the level of Rac1 activity within a cell can act as a switch to regulate the overall intrinsic pattern of cell migration. They proposed that at least four different stages of Rac1 activity might exist to differentially regulate the rate and pattern of intrinsic cell migration. With very little (stage 1) or very high (stage 4) levels of active Rac1, cells become immobilized, whereas moderate increase of Rac1 activity (stage 2) promotes the formation of a stabilized single lamella and directional movement, and is an ideal stage of Rac1 activation for cells in vivo. The further elevation of Rac1 activity results in stage 3, which is characterized by the formation of multiple lamellipodia around the cell periphery, and random migration. In line with these findings, we found that the level of Rac1 activity was higher in the ΔSt3 MEFs under various conditions compared with levels in WT MEFs (Fig. 3). This mimics the phenotype at stage 3 described above. Furthermore, consistent with the function of Rac1 in mediating membrane ruffles during cell spreading (Ridley and Hall, 1992; Price et al., 1998), we observed that the ΔSt3 MEFs exhibited more membrane ruffling when compared with WT cells during cell spreading on fibronectin (supplementary material Fig. S3).

Despite a difference in the level of formation of stress fibers between WT and ΔSt3 MEFs (Fig. 1B and Fig. 2A), we found that the basal level of RhoA activity was similar in both cell types. Thus, this excludes the possibility that the decrease of stress fiber formation in the ΔSt3 cells is due any reduction of GTP-RhoA (Fig. 3B). Furthermore, by inhibiting the activity of either Rac1 or its effector, PAK (Fig. 4C,D), we confirmed that the reduced stress fiber formation in ΔSt3 MEFs was a result of elevation of GTP-Rac1. By contrast, the expression of GFP-V12A- Rac1 (constitutively active mutant) in WT MEFs resulted in random migration as well as defective lamella formation and multiple protrusion (Fig. 4A,B; supplementary material Movie 6), which were similar phenotypes to those observed in the ΔSt3 MEFs (Fig. 1D,E; supplementary material Movie 4). These data suggest that the elevation of Rac1 activity is directly responsible for the loss of

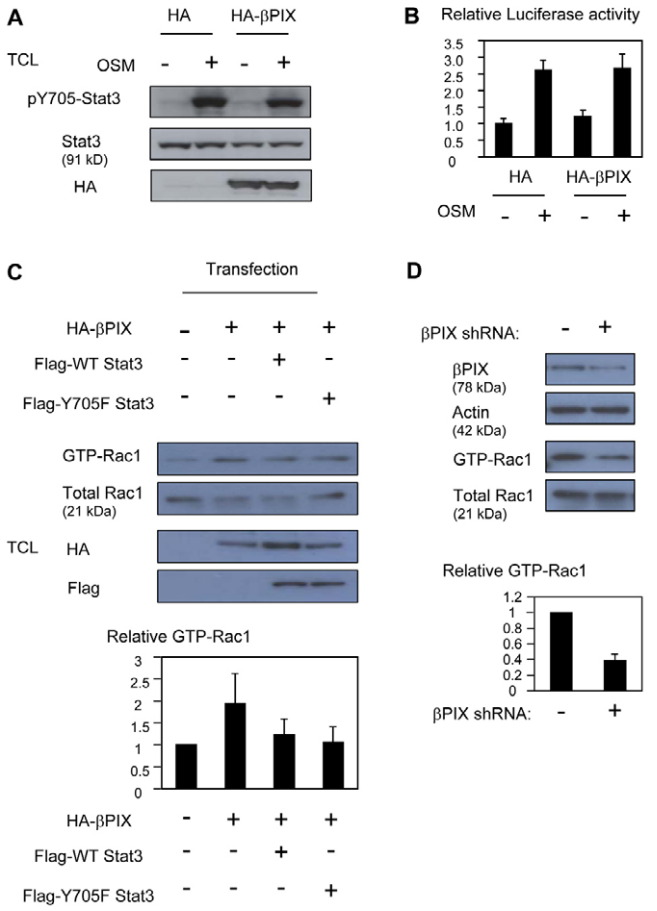

Fig. 7. Stat3 affects Rac1 regulation via its interaction with βPIX**.** (A,B) Effect of βPIX expression on Stat3 signaling. HEK293T cells were transfected with either HA vector or HA-βPIX in the presence of Stat3 luciferase reporter construct m67luc. Transfected cells were serum-starved and stimulated with OSM (10 ng/ml) for 8 hours before lysis. The phosphorylated Stat3 (pY705-Stat3), total Stat3 and HA-βPIX expression of the samples in A were analyzed by western blotting with the antibodies indicated. (B) Luciferase activity was performed to determine the transcriptional activity of endogenous Stat3. Data represent means ± s.e.m. (error bars), *n*=3. (C) Stat3 attenuates Rac1 activation induced by βPIX overexpression. HEK293T cells were cotransfected with HA-βPIX and FLAG vector or FLAG-Stat3 plasmids as indicated. The cells were then serum-starved for 24 hours before replating onto fibronectin-coated plates. Cells were assayed for Rac1 activity 1 hour after replating. The amount of GTP-Rac1 and total Rac1 were determined as described in the Materials and Methods. Data represent means ± s.e.m. (error bars), *n*=3. The expression of various proteins was tested in TCL using antibodies indicated.
(D) Knockdown of βPIX expression in ΔSt3 MEFs decreases Rac1 activation. The level of Rac1 activity was examined in ΔSt3 MEFs stably expressing βPIX shRNA or control vector 30 minutes after replating onto fibronectin. The level of βPIX expression was determined by western blot. The membrane was reprobed with anti-actin to serve as loading control. The amount of GTP-Rac1 and total Rac1 were determined as described in the Materials and Methods. Data represent means ± s.e.m. (error bars), *n*=3.

directional persistence during migration of the ΔSt3 MEFs, and that Stat3 has an important role in the regulation of Rac1 activity.

Focal adhesion kinase (FAK) is among the first proteins to be activated upon integrin signaling and has been reported to mediate Rac1 activation following integrin-extracellular matrix interaction (Cary et al., 1998; Hsia et al., 2003). We analyzed the level FAK activation during cell spreading on fibronectin and found that the level of FAK activity indicated by phosphorylation at Y397 was comparable between the WT and ΔSt3 MEFs (supplementary material Fig. S4). This suggests that other signaling pathways downstream of integrin, at least at the level of FAK, are not affected in the ΔSt3 MEFs.

βPIX, a Rac1/Cdc42 GEF, was first identified as a PAK-interacting protein (Bagrodia et al., 1998; Manser et al., 1998) and has been subsequently shown to mediate cell migration by regulating membrane ruffling, focal adhesion formation, cell polarity and reorganization of the actin cytoskeleton (Osmani et al., 2006; ten Klooster et al., 2006; Chang et al., 2007). Notably, βPIX can specifically bind to Rac1 in a nucleotide-independent manner and this interaction is sufficient to mediate the targeting and activation of Rac1 to the focal adhesions and membrane ruffles during cell spreading.

In addition to PAK, βPIX can bind to GIT1 to form a complex that mediates Rac1 activation (Bagrodia et al., 1999; Zhao et al., 2000). In light of these findings, we asked whether Stat3 could possibly interact with βPIX to affect Rac1 regulation. Indeed, we detected an endogenous association between Stat3 and βPIX (Fig. 6A), and this association was not dependent on the binding of PAK and GIT1 to βPIX. The coiled-coil domain of βPIX is required to mediate the oligomerization of βPIX (Kim et al., 2001), as well as being essential to the formation of membrane ruffles through Rac1 activation (Koh et al., 2001). Since we observed that both WT and Y705F Stat3 were able to bind to the truncated mutant of βPIX lacking the coiled-coil domain (Fig. 6E), Stat3 might bind to the monomeric form of βPIX. Thus, we speculate that the binding of Stat3 to βPIX might affect βPIX oligomerization to result in suppression of βPIX-induced Rac1 activation. In support of this notion, we demonstrated that overexpression of either WT or Y705F Stat3 was able to suppress Rac1 activation stimulated by βPIX overexpression (Fig. 7C).

Directional migration is a dynamic process regulated by the cytoskeletal machinery. Therefore, we postulated that it is more likely for Stat3 to function at the cytoplasmic level, or independently of mediating gene transcription, to regulate cell migration. In this study, we show that Y705F Stat3, a classical transcriptionally defective mutant that is primarily localized in the cytoplasm, can rescue the migratory defects of ΔStat3 MEFs in both wound healing and random cell migration by downregulation of Rac1 activity (Fig. 5). More importantly, we demonstrate that the suppression of βPIX expression in ΔSt3 MEFs by shRNA leads to a decrease in adhesion-induced Rac1 activation (Fig. 7D). This confirms that βPIX is a key regulator of Rac1 activation during cell adhesion and cell migration and that Stat3 exerts it regulation of Rac1 activity through the βPIX-Rac1 pathway. However, the question of how exactly the Stat3-βPIX interaction affects Rac1 activity remains to be answered. βPIX is targeted to the membrane ruffles and lamellipodia, where Rac1 is preferentially activated (ten Klooster et al., 2006). In our preliminary immunofluorescence analysis, we observed that the colocalization of βPIX with Rac1 at the membrane ruffles and lamellipodia seems to be higher in the migrating ΔSt3 MEFs than in WT MEFs (data not shown). Furthermore, although we showed that Stat3 can bind to βPIX independently of PAK, Rac1 and GIT1, the possibility of Stat3 associating with the whole βPIX-PAK-GIT1 complex to regulate Rac1 activity cannot be excluded. These issues require further investigation.

Previous studies have shown that the compromised migration in Stat3-deficient keratinocytes is partially due to the abnormal phosphorylation of $p130^{CAS}$ that contributes to the formation of focal adhesions (Kira et al., 2002). Stat3 has also been shown to interact with FAK and paxillin (Silver et al., 2004). Furthermore, transcriptional

activation of Stat3 target genes that promote migration or invasion, such as LIV-1 and matrix metalloproteinase 2 (MMP2), as well as MMP1 and MMP10, has also been reported (Xie et al., 2004; Yamashita et al., 2004; Itoh et al., 2006). Although the underlying mechanism coordinating these events is not fully understood, our data, together with these reports, reveal fundamental functions of Stat3 that are extensively involved in the control of cytoskeletal networks, cell adhesion, extracellular matrix and cell-cell interaction through transcription-dependent and -independent manners.

In conclusion, in this study, we present a novel cytoplasmic function of non-phosphorylated Stat3 in the direct regulation of directional cell migration by modulating Rac1 activity via an interaction with βPIX. Further studies are imperative for elucidating the essential function of Stat3 in tumor-cell invasion and metastasis on the basis of these novel findings on the cell migration and adhesion of mouse embryonic fibroblasts.

Materials and Methods

Cell culture, transfection and retroviral infection

MEFs and HeLa cells were cultured in Dulbecco's modified Eagle's medium (DMEM) containing 10% FBS and supplemented with penicillin-streptomycin and L-glutamine. MCF-7 and HEK293T cells were cultured in RPMI-1640 medium containing 10% FBS and supplemented with penicillin-streptomycin and L-glutamine. Transient transfections were performed with Lipofectamine 2000 (Invitrogen) according to the manufacturer's protocol. Generation of recombinant retroviruses and infection of cells were performed according to manufacturer's protocol (Clonetech). In brief, EcoPak 293 packaging cell line was transfected with the respective plasmid using Lipofectamine 2000. The supernatant containing the viral particles was collected 48 hours after transfection and used for infection of WT and ΔSt3 MEFs. After overnight incubation, the medium was replaced with fresh medium. Selection was performed 24 hours later using medium supplemented with geneticin (400 μg/ml).

Antibodies, chemicals and reagents

Antibodies against Stat3, phospho-Y705 Stat3, FAK and phospho-Y397 FAK were purchased from BD Biosciences. Antibodies against βPIX were purchased from Cell Signaling and Millipore. Antibodies against Rac1, acetylated α-tubulin, FLAG and HA were from Upstate Biotechnology, Zymed Laboratories, Sigma and Santa Cruz Biotechnology, respectively. Human plasma fibronectin, taxol, nocodazole and phorbol 12-myristate 13-acetate (PMA) were purchased from Sigma. Alexa Fluor 488 and Texas Red-X phalloidin were from Invitrogen.

Plasmid construction, siRNAs and shRNA

pLEGFP-C1 (Clonetech) vector inserted with murine Stat3 cDNA was used as template for the generation of Y705F Stat3 using site-directed mutagenesis, in which the Y705 was point-mutated to F. For the generation of GFP-tagged Rho GTPase mutants, cDNA encoding for G12V-Rac1, T17N-Rac1 and G14V-RhoA were first amplified from the respective pXJ40 HA constructs by PCR before being subcloned into pLEGFP-C1 vector using *Xho*I and *Hin*dIII restriction enzymes. All constructs were checked by full-length sequencing to verify point mutations. The various Stat3 and βPIX mutant plasmids have been described previously (Manser et al., 1998; Zhang et al., 2000; Loo et al., 2004). The expression vectors encoding the siRNAs were constructed by ligating the target sequences containing annealed oligonucleotides into pSilencer 2.1-U6 neo (Ambion) according to the manufacturer's instructions. The double-stranded oligonucleotides used to construct the human STAT3 siRNA expression vector were 5′-GATCCGGGTCCAGTTCACTACTATTCAAGAGAT-AGTAGTGAACTGGACGCCTTTTTTGGAAA-3′ and 5′-GCTTTTCCAAAAA-AGGCGTCCAGTTCACTACTATCTCTTGAATAGTAGTGAACTGGACGCCG-3′. A Basic Alignment Search Tool search of all target sequences showed no significant sequence homology with other genes. All siRNA expression vectors were confirmed by sequence analysis of the target insert. Stable cell lines were then established from cells transfected with pSilencer 2.1-U6 neo expression vector expressing the siRNA by selecting with neomycin according to manufacturer's recommendations.

The pLK.1-puro plasmid containing the βPIX shRNA sequence 3′-CCGGCCT-GAAGGTTATCGAAGCTTACTCGAGTAAGCTTCGATAACCTTCAGGTTTTTG-5′ (clone: NM_017402.2-1997s1c1) and control pLK.1-puro plasmid vector were purchased from Sigma. ΔSt3 MEFs were transfected with either plasmid and selected with puromycin.

Cell migration analysis

For all cell migration analysis, cells were seeded on dishes coated with human plasma fibronectin. For wound healing assays, 0.75×10^6 cells were seeded on 60 mm dishes. The cells were then serum-starved and treated with mitomycin C (10 μg/ml) for 2 hours to inhibit cell division. Wounding was induced by scratching the monolayer with a micropipette tip and the dish was placed in a temperature- and CO_2-controlled chamber of the Leica DMIRE2 inverted microscope. Phase-contrast images were collected using either 10× or 20× objective lenses for a period of 16-24 hours with a CCD video camera (Leica DC 500). For random migration assay, 0.15×10^4 cells were seeded on 60 mm dishes and cultured overnight before similarly being treated with mitomycin C. Cell migration was monitored by time-lapse microscopy (Leica DMIRE2) using 5× and 10× objective lenses. Phase-contrast images were collected at every 15 minutes for a period of 12-16 hours with a CCD video camera (Leica DC 500). The images collected were stored as stacks using the Axiovision software (Carl Zeiss Imaging Solutions) to quantify migratory parameters including the migration distance, rate, path and directional persistence. For quantification, cells were manually tracked for each frame based on the central position of the nuclei. Directional persistence was represented by the ratio of the shortest linear direct distance from the start to the end point divided by the total track distance migrated by an individual cell. Migration rate was defined by the total distance traveled divided by time and expressed in units of μm/hour. Based on the coordinates obtained from the translocation of the nuclei of the cells, graphical representations of the migratory paths were generated using Excel for visualization.

Immunofluorescence

All cells were seeded on fibronectin-coated coverslips for immunofluorescence staining. Cells were fixed with 4% paraformaldehyde in PEM (80 mM PIPES pH 6.8, 5 mM EGTA and 2 mM $MgCl_2$), permeabilized in 0.2% Triton X-100 in PBS and blocked with 10% FBS in PBS. Cell were incubated with the indicated primary antibodies in 1% BSA in PBS followed by incubation with the appropriate secondary antibodies conjugated with either Alexa Fluor 488 (Molecular Probes) or Cy3 (Invitrogen). Cells were washed, mounted and examined with confocal laser-scanning microscope (Fluoview FV100; Olympus) using 60× NA 1.42 objective. Images were collected using FV10-ASW software and processed with Adobe Photoshop software.

Measurement of Rho GTPase activity

To determine Rac1 activity during cell spreading, cells were serum-starved overnight and detached with 0.0625% trypsin and 5 mM EDTA. Detached cells were then suspended in serum-free medium for 60-90 minutes before being replated onto fibronectin for the time indicated. For measurement of Rac1 activity in migrating cells, migration was stimulated by making 40 scratches on a confluent monolayer. At the time indicated, cells were washed with PBS and lyzed for 5 minutes in lysis buffer containing 25 mM Tris-HCl, pH 7.5, 150 mM NaCl, 5 mM $MgCl_2$, 1% NP40, 1 mM DTT, 5% glycerol and protease inhibitor cocktail. Cell lysates were clarified by centrifugation at 16,100 ***g*** for 5 minutes. The lysate was incubated with GST-CRIB domain of PAK (20 μg) at 4°C for 30 minutes before further incubation with glutathione-Sepharose 4B beads at 4°C for 30 minutes. The level of GTP-bound Rac1 was analyzed by SDS-PAGE and western blotting with anti-Rac1 antibody. Densitometry analysis was performed with NIH ImageJ software and the level of GTP-Rac1 was normalized against the total amount of Rac1 present in the cell lysate before being expressed as relative fold of GTP-Rac1 compared with WT MEFs. RhoA G-LISA activation assay kits (Cytoskeleton) were used to measure the level of GTP-RhoA according to manufacturer's protocol.

Immunoprecipitation and immunoblotting

Transfected or untransfected cells were washed once with PBS and lysed for 5 minutes with lysis buffer containing 20 mM Tris-HCl, pH 7.4, 1 mM EDTA, 50 mM KCL, 1 mM DTT, 10 mM Na_3VO_4, 5 mM $MgCl_2$, 5 mM NaF, 10% glycerol, 1% Triton X-100 and protease inhibitors. Cell lysates were prepared for immunoprecipitation and western blotting as previously described (Lufei et al., 2003)

Luciferase assay

Cells seeded on 24-well dishes were transfected with firefly luciferase reporter gene construct and the required expression plasmid, together with the thymidine kinase promoter-dependent *Renilla* luciferase construct (Promega), which was used as an internal control for transfection efficiency. Cells were serum-starved overnight at 48 hours after transfection, before stimulation with OSM (10 ng/ml) for 8 hours and prepared as previously described (Lufei et al., 2003).

Statistical analysis

For statistical analysis, data were analyzed using Student's *t*-test and $P<0.05$ was interpreted as statistically significant.

This work was supported by the Agency for Science, Technology and Research of Singapore. E.M. is supported by the GSK-IMCB Singapore research fund. We thank C. P. Lim for reading the manuscript.

References

Abdulghani, J., Gu, L., Dagvadorj, A., Lutz, J., Leiby, B., Bonuccelli, G., Lisanti, M. P., Zellweger, T., Alanen, K., Mirtti, T. et al. (2008). Stat3 promotes metastatic progression of prostate cancer. *Am. J. Pathol.* **172**, 1717-1728.

Albertinazzi, C., Cattelino, A. and de Curtis, I. (1999). Rac GTPases localize at sites of actin reorganization during dynamic remodeling of the cytoskeleton of normal embryonic fibroblasts. *J. Cell Sci.* **112**, 3821-3831.

Bagrodia, S., Taylor, S. J., Jordon, K. A., Van Aelst, L. and Cerione, R. A. (1998). A novel regulator of p21-activated kinases. *J. Biol. Chem.* **273**, 23633-23636.

Bagrodia, S., Bailey, D., Lenard, Z., Hart, M., Guan, J. L., Premont, R. T., Taylor, S. J. and Cerione, R. A. (1999). A tyrosine-phosphorylated protein that binds to an important regulatory region on the cool family of p21-activated kinase-binding proteins. *J. Biol. Chem.* **274**, 22393-22400.

Bernards, A. (2003). GAPs galore! A survey of putative Ras superfamily GTPase activating proteins in man and Drosophila. *Biochim. Biophys. Acta.* **1603**, 47-82.

Bowman, T., Garcia, R., Turkson, J. and Jove, R. (2000). STATs in oncogenesis. *Oncogene* **19**, 2474-2488.

Bromberg, J. F., Horvath, C. M., Besser, D., Lathem, W. W. and Darnell, J. E., Jr. (1998). Stat3 activation is required for cellular transformation by v-src. *Mol. Cell. Biol.* **18**, 2553-2558.

Calo, V., Migliavacca, M., Bazan, V., Macaluso, M., Buscemi, M., Gebbia, N. and Russo, A. (2003). STAT proteins: from normal control of cellular events to tumorigenesis. *J. Cell Physiol.* **197**, 157-168.

Cary, L. A., Han, D. C., Polte, T. R., Hanks, S. K. and Guan, J. L. (1998). Identification of p130Cas as a mediator of focal adhesion kinase-promoted cell migration. *J. Cell Biol.* **140**, 211-221.

Chang, F., Lemmon, C. A., Park, D. and Romer, L. H. (2007). FAK potentiates Rac1 activation and localization to matrix adhesion sites: a role for betaPIX. *Mol. Biol. Cell* **18**, 253-264.

Cory, G. O. and Ridley, A. J. (2002). Cell motility: braking WAVEs. *Nature* **418**, 732-733.

Costa-Pereira, A. P., Tininini, S., Strobl, B., Alonzi, T., Schlaak, J. F., Is'harc, H., Gesualdo, I., Newman, S. J., Kerr, I. M. and Poli, V. (2002). Mutational switch of an IL-6 response to an interferon-gamma-like response. *Proc. Natl. Acad. Sci. USA* **99**, 8043-8047.

Darnell, J. E., Jr. (1997). STATs and gene regulation. *Science* **277**, 1630-1635.

Darnell, J. E., Jr., Kerr, I. M. and Stark, G. R. (1994). Jak-STAT pathways and transcriptional activation in response to IFNs and other extracellular signaling proteins. *Science* **264**, 1415-1421.

Debidda, M., Wang, L., Zang, H., Poli, V. and Zheng, Y. (2005). A role of STAT3 in Rho GTPase-regulated cell migration and proliferation. *J. Biol. Chem.* **280**, 17275-17285.

Hsia, D. A., Mitra, S. K., Hauck, C. R., Streblow, D. N., Nelson, J. A., Ilic, D., Huang, S., Li, E., Nemerow, G. R., Leng, J. et al. (2003). Differential regulation of cell motility and invasion by FAK. *J. Cell Biol.* **160**, 753-767.

Itoh, M., Murata, T., Suzuki, T., Shindoh, M., Nakajima, K., Imai, K. and Yoshida, K. (2006). Requirement of STAT3 activation for maximal collagenase-1 (MMP-1) induction by epidermal growth factor and malignant characteristics in T24 bladder cancer cells. *Oncogene* **25**, 1195-1204.

Kaptein, A., Paillard, V. and Saunders, M. (1996). Dominant negative stat3 mutant inhibits interleukin-6-induced Jak-STAT signal transduction. *J. Biol. Chem.* **271**, 5961-5964.

Katoh, H., Hiramoto, K. and Negishi, M. (2006). Activation of Rac1 by RhoG regulates cell migration. *J. Cell Sci.* **119**, 56-65.

Kim, S., Lee, S. H. and Park, D. (2001). Leucine zipper-mediated homodimerization of the p21-activated kinase-interacting factor, beta Pix. Implication for a role in cytoskeletal reorganization. *J. Biol. Chem.* **276**, 10581-10584.

Kira, M., Sano, S., Takagi, S., Yoshikawa, K., Takeda, J. and Itami, S. (2002). STAT3 deficiency in keratinocytes leads to compromised cell migration through hyperphosphorylation of p130(cas). *J. Biol. Chem.* **277**, 12931-12936.

Koh, C. G., Manser, E., Zhao, Z. S., Ng, C. P. and Lim, L. (2001). Beta1PIX, the PAK-interacting exchange factor, requires localization via a coiled-coil region to promote microvillus-like structures and membrane ruffles. *J. Cell Sci.* **114**, 4239-4251.

Kozma, R., Ahmed, S., Best, A. and Lim, L. (1995). The Ras-related protein Cdc42Hs and bradykinin promote formation of peripheral actin microspikes and filopodia in Swiss 3T3 fibroblasts. *Mol. Cell. Biol.* **15**, 1942-1952.

Lauffenburger, D. A. and Horwitz, A. F. (1996). Cell migration: a physically integrated molecular process. *Cell* **84**, 359-369.

Levy, D. E. and Lee, C. K. (2002). What does Stat3 do? *J. Clin. Invest.* **109**, 1143-1148.

Lim, C. P., Phan, T. T., Lim, I. J. and Cao, X. (2006). Stat3 contributes to keloid pathogenesis via promoting collagen production, cell proliferation and migration. *Oncogene* **25**, 5416-5425.

Loo, T. H., Ng, Y. W., Lim, L. and Manser, E. (2004). GIT1 activates p21-activated kinase through a mechanism independent of p21 binding. *Mol. Cell. Biol.* **24**, 3849-3859.

Lufei, C., Ma, J., Huang, G., Zhang, T., Novotny-Diermayr, V., Ong, C. T. and Cao, X. (2003). GRIM-19, a death-regulatory gene product, suppresses Stat3 activity via functional interaction. *EMBO J.* **22**, 1325-1335.

Manser, E., Loo, T. H., Koh, C. G., Zhao, Z. S., Chen, X. Q., Tan, L., Tan, I., Leung, T. and Lim, L. (1998). PAK kinases are directly coupled to the PIX family of nucleotide exchange factors. *Mol. Cell* **1**, 183-192.

Ng, D. C., Lin, B. H., Lim, C. P., Huang, G., Zhang, T., Poli, V. and Cao, X. (2006). Stat3 regulates microtubules by antagonizing the depolymerization activity of stathmin. *J. Cell Biol.* **172**, 245-257.

Nobes, C. D. and Hall, A. (1995). Rho, rac, and cdc42 GTPases regulate the assembly of multimolecular focal complexes associated with actin stress fibers, lamellipodia, and filopodia. *Cell* **81**, 53-62.

Nobes, C. D. and Hall, A. (1999). Rho GTPases control polarity, protrusion, and adhesion during cell movement. *J. Cell Biol.* **144**, 1235-1244.

Osmani, N., Vitale, N., Borg, J. P. and Etienne-Manneville, S. (2006). Scrib controls Cdc42 localization and activity to promote cell polarization during astrocyte migration. *Curr. Biol.* **16**, 2395-2405.

Pankov, R., Endo, Y., Even-Ram, S., Araki, M., Clark, K., Cukierman, E., Matsumoto, K. and Yamada, K. M. (2005). A Rac switch regulates random versus directionally persistent cell migration. *J. Cell Biol.* **170**, 793-802.

Pollard, T. D. and Borisy, G. G. (2003). Cellular motility driven by assembly and disassembly of actin filaments. *Cell* **112**, 453-465.

Pratt, S. J., Epple, H., Ward, M., Feng, Y., Braga, V. M. and Longmore, G. D. (2005). The LIM protein Ajuba influences p130Cas localization and Rac1 activity during cell migration. *J. Cell Biol.* **168**, 813-824.

Price, L. S., Leng, J., Schwartz, M. A. and Bokoch, G. M. (1998). Activation of Rac and Cdc42 by integrins mediates cell spreading. *Mol. Biol. Cell* **9**, 1863-1871.

Raftopoulou, M. and Hall, A. (2004). Cell migration: Rho GTPases lead the way. *Dev. Biol.* **265**, 23-32.

Ridley, A. J. (2001). Rho GTPases and cell migration. *J. Cell Sci.* **114**, 2713-2722.

Ridley, A. J. and Hall, A. (1992). The small GTP-binding protein rho regulates the assembly of focal adhesions and actin stress fibers in response to growth factors. *Cell* **70**, 389-399.

Ridley, A. J., Paterson, H. F., Johnston, C. L., Diekmann, D. and Hall, A. (1992). The small GTP-binding protein rac regulates growth factor-induced membrane ruffling. *Cell* **70**, 401-410.

Ridley, A. J., Schwartz, M. A., Burridge, K., Firtel, R. A., Ginsberg, M. H., Borisy, G., Parsons, J. T. and Horwitz, A. R. (2003). Cell migration: integrating signals from front to back. *Science* **302**, 1704-1709.

Rossman, K. L., Der, C. J. and Sondek, J. (2005). GEF means go: turning on RHO GTPases with guanine nucleotide-exchange factors. *Nat. Rev. Mol. Cell. Biol.* **6**, 167-180.

Sander, E. E., ten Klooster, J. P., van Delft, S., van der Kammen, R. A. and Collard, J. G. (1999). Rac downregulates Rho activity: reciprocal balance between both GTPases determines cellular morphology and migratory behavior. *J. Cell Biol.* **147**, 1009-1022.

Sanders, L. C., Matsumura, F., Bokoch, G. M. and de Lanerolle, P. (1999). Inhibition of myosin light chain kinase by p21-activated kinase. *Science* **283**, 2083-2085.

Sano, S., Itami, S., Takeda, K., Tarutani, M., Yamaguchi, Y., Miura, H., Yoshikawa, K., Akira, S. and Takeda, J. (1999). Keratinocyte-specific ablation of Stat3 exhibits impaired skin remodeling, but does not affect skin morphogenesis. *EMBO J.* **18**, 4657-4668.

Schlenker, O. and Rittinger, K. (2009). Structures of dimeric GIT1 and trimeric beta-PIX and implications for GIT-PIX complex assembly. *J. Mol. Biol.* **386**, 280-289.

Silver, D. L., Naora, H., Liu, J., Cheng, W. and Montell, D. J. (2004). Activated signal transducer and activator of transcription (STAT) 3, localization in focal adhesions and function in ovarian cancer cell motility. *Cancer Res.* **64**, 3550-3558.

Silver, D. L., Geisbrecht, E. R. and Montell, D. J. (2005). Requirement for JAK/STAT signaling throughout border cell migration in Drosophila. *Development* **132**, 3483-3492.

Simon, A. R., Vikis, H. G., Stewart, S., Fanburg, B. L., Cochran, B. H. and Guan, K. L. (2000). Regulation of STAT3 by direct binding to the Rac1 GTPase. *Science* **290**, 144-147.

Takeda, K., Noguchi, K., Shi, W., Tanaka, T., Matsumoto, M., Yoshida, N., Kishimoto, T. and Akira, S. (1997). Targeted disruption of the mouse Stat3 gene leads to early embryonic lethality. *Proc. Natl. Acad. Sci. USA* **94**, 3801-3804.

ten Klooster, J. P., Jaffer, Z. M., Chernoff, J. and Hordijk, P. L. (2006). Targeting and activation of Rac1 are mediated by the exchange factor beta-Pix. *J. Cell Biol.* **172**, 759-769.

Wei, D., Le X., Zheng, L., Wang, L., Frey, J. A., Gao, A. C., Peng, Z., Huang, S., Xiong, H. Q., Abbruzzese, J. L. et al. (2003). Stat3 activation regulates the expression of vascular endothelial growth factor and human pancreatic cancer angiogenesis and metastasis. *Oncogene* **22**, 319-329.

Xie, T. X., Wei, D., Liu, M., Gao, A. C., Ali-Osman, F., Sawaya, R. and Huang, S. (2004). Stat3 activation regulates the expression of matrix metalloproteinase-2 and tumor invasion and metastasis. *Oncogene* **23**, 3550-3560.

Yamashita, S., Miyagi, C., Carmany-Rampey, A., Shimizu, T., Fujii, R., Schier, A. F. and Hirano, T. (2002). Stat3 controls cell movements during zebrafish gastrulation. *Dev. Cell* **2**, 363-375.

Yamashita, S., Miyagi, C., Fukada, T., Kagara, N., Che, Y. S. and Hirano, T. (2004). Zinc transporter LIVI controls epithelial-mesenchymal transition in zebrafish gastrula organizer. *Nature* **429**, 298-302.

Zhang, T., Kee, W. H., Seow, K. T., Fung, W. and Cao, X. (2000). The coiled-coil domain of Stat3 is essential for its SH2 domain-mediated receptor binding and subsequent activation induced by epidermal growth factor and interleukin-6. *Mol. Cell. Biol.* **20**, 7132-7139.

Zhao, Z. S., Manser, E., Chen, X. Q., Chong, C., Leung, T. and Lim, L. (1998). A conserved negative regulatory region in alphaPAK: inhibition of PAK kinases reveals their morphological roles downstream of Cdc42 and Rac1. *Mol. Cell. Biol.* **18**, 2153-2163.

Zhao, Z. S., Manser, E., Loo, T. H. and Lim, L. (2000). Coupling of PAK-interacting exchange factor PIX to GIT1 promotes focal complex disassembly. *Mol. Cell. Biol.* **20**, 6354-6363.